Available online at www.sciencedirect.com

ScienceDirect

Chinese Journal of Aeronautics 22(2009) 113-120

Chinese Journal of Aeronautics

www.elsevier.com/locate/cja

Prediction of Boundary Layer Transition Based on Modeling of Laminar Fluctuations Using RANS Approach

Reza Taghavi Z., Mahmood Salary, Amir Kolaei*

Department of Mechanical Engineering, Iran University of Science and Technology, Tehran 16846, Iran

Received 12 November 2007; accepted 10 December 2008

Abstract

This article presents a linear eddy-viscosity turbulence model for predicting bypass and natural transition in boundary layers by using Reynolds-averaged Navier-Stokes (RANS) equations. The model includes three transport equations, separately, to compute laminar kinetic energy, turbulent kinetic energy, and dissipation rate in a flow field. It needs neither correlations of intermittency factors nor knowledge of the transition onset. Two transition tests are carried out: flat plate boundary layer under zero and non-zero pressure gradients with different freestream turbulence intensities, and transitional flow over a wind turbine blade at a chord Reynolds number of 3×10^6. Results are presented in terms of skin friction coefficients. Comparison with the experimental data from both tests evidences a good agreement there is between them.

Keywords: boundary layer transition; eddy-viscosity turbulence model; laminar fluctuations

1. Introduction

Predicting the onset of boundary layer transition is one of the most important concerns in fluid mechanics. As a common transition phenomenon, transitional flows can be observed on a significant part of blades in low-pressure gas turbines. Other examples of importance may be cited as the same flow moving over wings and bodies of airplanes, which will exert enormous effects upon the aerodynamic characteristics. In transitional regions, the heat transfer rate and wall shear stress have sharp rise, making an accurate design of gas turbine blades based on heat loads and shear forces possible only after the mechanism and features of boundary layer transition have been fully understood.

Boundary layer flow over different objects may happen with different modes of transition mainly depending on their geometry and flow conditions. For flows with very low intensity of freestream turbulence, their fluctuations are quite similar with Tollmien-Schlichting (T-S) waves, of which the linear growth can be explained by the linear stability theory[1]. Usually regarded as 'natural transition', the transition to turbulence through this mechanism is a slow process[2], which often takes place on the bodies of flying objects. At an order upwards of 1% freestream turbulence intensity, it is observed experimentally that transition occurs abruptly and deviates from the linear growth of T-S waves. In this case, turbulent spots appear at the beginning of the transition region. This phenomenon is termed 'bypass transition' and considered to be usual on gas turbine blades[3].

Centred on such an important phenomenon, little successes were achieved in its simulation due to some detrimental influences from factors like short length of transition zone with rapid variation of flow parameters in it. Therefore, most results were acquired either from experiments or from direct numerical simulation by using supercomputer. However, in the recent decade, an extensive attempt has been made to explore common industrial methods, such as Reynolds-averaged Navier-Stokes (RANS), to clarify the flow behaviours in the transitional region.

There are mainly two approaches used to model bypass transition in industry. The first is to apply low-Reynolds number turbulence models[4-5], in which wall-damping functions integrated into turbulent transport equations are used to determine the onset of boundary layer transition. This can be implanted into existing CFD codes with great ease. However, experience has indicated the inability of this approach to reliably reflect the influences of all factors that affect the transition such as freestream turbulence, pressure gradients and wall roughness[6]. In addition, there is no

*Corresponding author. Tel.: +98-711-2341158.
E-mail address: kdaei@mail.iust.ac.ir

doi: 10.1016/S1000-9361(08)60076-X

inherent reason, why damping functions, which have been optimized to damp the turbulence in the viscous sub-layer, should reliably predict an entirely different and complex physical process.

The second is to use experimental correlations, which usually relate the freestream turbulence intensity, to the transition Reynolds number based on the momentum-thickness. Typical examples are the models presented by R. E. Mayle[7] and B. J. Abu-Ghannam, et al.[8], which are based on their experimental observations. While this approach proves sufficiently accurate, it poses numerical and programming challenges to Navier-Stokes methods. The most important problem is the necessity of comparing actual momentum-thickness Reynolds numbers with its critical value derived from the correlations in the numerical solution. This is not an easy task in Navier-Stokes environment because the boundary layer edge is not well defined and the integration will therefore depend on the details of the implementation of the search algorithm. This problem is further complicated by modern CFD methods based on unstructured grids and massive parallel execution.

This article aims to develop a physical model for predicting transitional flows. The model is based on simulation of laminar streamwise fluctuation, which usually exists in pre-transitional region of boundary layer and application of an eddy viscosity approach. For this purpose, is introduced a turbulence-transition model inclusive of three transport equations for laminar kinetic energy, turbulent kinetic energy, and dissipation rate. This model is established on the base of recent works of R. E. Mayle, et al.[9] and D. K. Walters, et al.[10]. This article also performs some tests to examine the capability of the physical model for predicting laminar-turbulent transition in boundary layers. As for advantages of this model, could be cited its independence from either correlations developed for intermittency factors[11-12] or specific position of transition onset.

2. Concepts

A boundary layer near the leading edge of a flat plate is subjected to the freestream turbulence very close to the Blasius form, whereas further downstream it starts to deviate so that an increased velocity is observed in the inner half of the boundary layer and a decrease in the outer half[13]. The increased velocity close to the wall means an increase in skin friction within the pre-transitional region compared to the Blasius boundary layer. This is accompanied by the development of relatively high-amplitude streamwise fluctuations, which can reach an intensity several times the level of freestream turbulence[14]. R. E. Mayle, et al.[9] suggested a theory for calculating these streamwise fluctuations in terms of laminar kinetic energy as distinct structurally from turbulent fluctuations. D. K. Walters, et al.[10] added a transport equation to the k-ε turbulence model so as to consider laminar kinetic energy denoted by k_l similar to the turbulent kinetic energy by k_t. Thus, the model used in this study also contains three transport equations for k_l, k_t, and far field dissipation rate, ε.

Growth of the laminar kinetic energy is explained by the splat mechanism proposed by P. Bradshaw[15] and discussed in more detail by R. J. Volino[16]. This mechanism suggests that the wall redirects the normal fluctuation into a streamwise component, and at the same time creates local pressure gradients in the boundary layer thus amplifying disturbance.

With the splat mechanism, it is assumed that the turbulent energy spectrum in the near wall region can be divided into wall-affected (large scale) and non-wall-affected (small scale) sections. Therefore, the small scale component of k_t is denoted by $k_\mathrm{t,s}$, and the large scale component by $k_\mathrm{t,l}$. In the freestream, $k_\mathrm{t,s}$ approaches k_t and $k_\mathrm{t,l}$ zero.

In this model, predicting the onset of transition is based on a local parameter that depends on the turbulent energy and effective length scale. Once this parameter reaches a certain value, transition begins and energy from the streamwise fluctuations (k_l) converts into the turbulent fluctuations (k_t). The threshold values are separately defined for predicting natural or bypass transition. Down-stream of the transition zone, the model predicts a fully turbulent boundary layer.

The k_t, k_l, and ε transport equations in an incompressible form are as follows

$$\frac{\mathrm{d}k_\mathrm{t}}{\mathrm{d}t}=\frac{\partial}{\partial x_j}\left[\left(\nu+\frac{\alpha_\mathrm{t}}{\sigma_k}\right)\frac{\partial k_\mathrm{t}}{\partial x_j}\right]+P_\mathrm{t}+R+R_\mathrm{nat}-\varepsilon-D_\mathrm{t} \quad (1)$$

$$\frac{\mathrm{d}k_\mathrm{l}}{\mathrm{d}t}=\frac{\partial}{\partial x_j}\left(\nu\frac{\partial k_\mathrm{l}}{\partial x_j}\right)+P_\mathrm{l}-R-R_\mathrm{nat}-D_\mathrm{l} \quad (2)$$

$$\frac{\mathrm{d}\varepsilon}{\mathrm{d}t}=\frac{\partial}{\partial x_j}\left[\left(\nu+\frac{\alpha_\mathrm{t}}{\sigma_\varepsilon}\right)\frac{\partial \varepsilon}{\partial x_j}\right]+C_{\varepsilon 1}\frac{\varepsilon}{k_\mathrm{t}}\left(P_\mathrm{t}+R_\mathrm{nat}\right)+C_{\varepsilon R}R\frac{\varepsilon}{\sqrt{k_\mathrm{l}k_\mathrm{t}}}-C_{\varepsilon 2}\frac{\varepsilon^2}{k_\mathrm{t}}-\frac{\varepsilon}{k_\mathrm{t}}D_\mathrm{t} \quad (3)$$

where P_t and P_l, which represent the turbulent and laminar kinetic power, respectively, are defined as

$$P_\mathrm{t}=\nu_\mathrm{t,s}S^2 \quad (4)$$

$$P_\mathrm{l}=\nu_\mathrm{t,l}S^2 \quad (5)$$

where $\nu_\mathrm{t,l}$ and $\nu_\mathrm{t,s}$ are large scale and small scale turbulent kinematic viscosity, respectively, and S is the modulus of the mean strain-rate tensor.

R, the bypass transition production term, can be defined as

$$R=C_R\beta_\mathrm{bp}\frac{k_\mathrm{l}}{\tau_\mathrm{t}} \quad (6)$$

where τ_t is turbulent time scale.

R_{nat}, the natural transition production term, may be defined as

$$R_{nat} = C_{R,nat}\beta_{nat}k_l S \tag{7}$$

The threshold functions, β_{bp} and β_{nat}, govern the bypass and the natural transition, respectively.

D_t and D_l, the turbulent and laminar kinetic energy due to near-wall dissipation respectively, can be calculated by

$$D_t = 2\nu\frac{\partial\sqrt{k_t}}{\partial x_j}\frac{\partial\sqrt{k_t}}{\partial x_j} \tag{8}$$

$$D_l = 2\nu\frac{\partial\sqrt{k_l}}{\partial x_j}\frac{\partial\sqrt{k_l}}{\partial x_j} \tag{9}$$

The influences of turbulent and laminar fluctuations on the mean flow are taken into account by specifying the total eddy-viscosity.

$$-u_i u_j = \nu_{tot}\left(\frac{\partial U_i}{\partial x_j}+\frac{\partial U_j}{\partial x_i}\right)-\frac{2}{3}k_t\delta_{ij} \tag{10}$$

where

$$\nu_{tot} = \nu_{t,s} + \nu_{t,l} \tag{11}$$

For definitions of other parameters, refer to D. K. Walters, et al[10]. In this article, to predict the proper onset of transition, some of the model constants have been modified.

3. Flow Conditions and their Computational Implementation

This article considers seven different flow cases. The first six are boundary layers developing along a flat plate with sharp leading edge, of which three are developing under zero-pressure gradient, and the other three are under a variable pressure gradient, favorable upstream and adverse downstream. The flows over the flat plate accord with those in experiments[3]. Apart from pressure gradients, the flows also differ in inlet velocity and freestream turbulence intensity. Fig.1 shows the computational domains in these flat plate cases. The computational inlet extends a certain amount upstream of the flat plate leading edge, and a symmetry plane is applied at the bottom of the domain upstream of the leading edge. This allows for a natural stagnation of the freestream flow and boundary layer initiation. In the cases that are susceptible to be under variable pressure gradients, the gradients are caused by contouring the upper wall bounding the freestream and imposing the slip condition over it.

Geometries for zero-pressure gradient flat plate cases, T3A-, T3A, and T3B, are computed with a numerical grid made of 350×100 nodes, while for the variable pressure gradient case, T3Cx, a grid of 350×120. These meshes are chosen on the base of grid-independence studies.

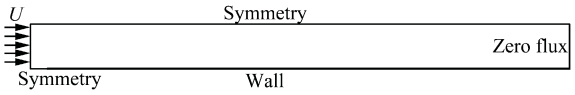

(a) T3A-, T3A, and T3B

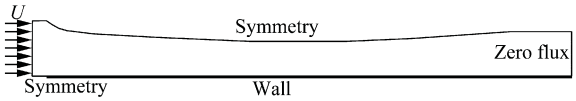

(a) T3Cx

Fig.1 Computational domains used for simulation.

The seventh case belongs to the transitional flow over a wind turbine blade denoted by the 'S809 blade'. The inlet freestream turbulence for this case is about 0.07 %, which usually produces the natural transition. Fig.2 illustrates a part of the domain mesh of the computational domain containing 45 000 nodes. Again, grid-independence tests have justified this choice.

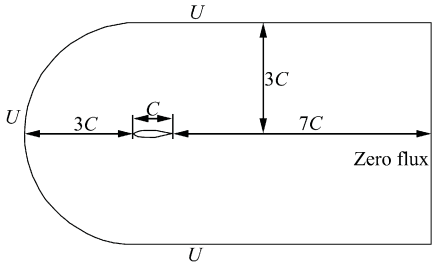

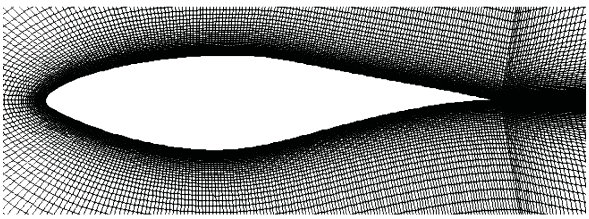

Fig.2 Computational domains and grids used for simulation of S809 blade.

Other details of computational conditions for each test are described in the relevant sections. The blade and the T3A- case are selected to examine the model for predicting turbulent transition under conditions of extremely low freestream turbulence, i.e. natural transition, which is a challenge to RANS approaches.

The model equations have been implemented with an in-house code, which uses the general non-orthogonal, segregated finite volume scheme. Conversion of all transported properties is approximated by the second-order upwind scheme. Mass conservation is enforced via the SIMPLE pressure-correction algorithm, which yields the correct pressure field by an iterative sequence and essentially nullifies the mass residuals in all computational cells.

4. Results and Discussion

This article studies the process of transition in terms of the friction coefficients along the stream-wise direction since, as a very sensitive indicator, the friction coefficient soars as soon as transition occurs.

4.1. Flat plate boundary layer under zero pressure gradients

The input data for the ongoing tests including upstream velocity of U, turbulent intensity level of Tu, and turbulent length scale of λ. Three cases are to be under investigation. Table 1 separately lists their above-cited input data. The inlet value of the laminar kinetic energy k_l, is reasonably assumed zero. The turbulent kinetic energy k_t, and turbulent dissipation rate ε, are determined by

$$k_t = \frac{3}{2}(\mathrm{Tu}\cdot U)^2 \tag{12}$$

$$\varepsilon = \frac{k_{\mathrm{tot}}^{3/2}}{\lambda} \tag{13}$$

Table 1 Inlet flow parameters for flat plate boundary layer flow with zero pressure gradient[3]

Test case	Tu/%	U/(m·s^{-1})	λ/mm
T3A-	0.9	19.8	2.0
T3A	3.0	5.4	9.0
T3B	6.0	9.4	4.5

Fig.3 shows the computational and experimental results of friction coefficients for T3A-, T3A, and T3B cases as a function of the Reynolds numbers on downstream position, *Re*. Note that the freestreams in T3A- case usually undergoes a natural transition while the high freestream in T3A and T3B cases is a pure bypass transition in the flow field. In the same figure, are also presented the friction coefficients for laminar flows and turbulent flows derived from the standard k-ε (SKE) and Menter's k-ω SST (KW-SST)[17] turbulence models for better comparison.

As seen in Fig.3, the results with the proposed method are in close agreement with the experimental results for both natural transition of T3A- and bypass transitions of T3A and T3B. The laminar pre-transition zone, the starting point of transition and the turbulent zone are modelled precisely. However, a slight overshoot can be found as distinct from the experimental results at the end of the transition zone, which might be attributed to the way the model reckons with the transfer of energy between k_l and k_t in the transitional region.

It is worth mentioning that in many engineering applications, predicting the onset of transition is more important than knowing other behaviours like transition length in transitional region, which is usually small enough to be unworthy of attention.

It is evident from Fig.3 that the standard k-ε and high-*Re* version of Menter's k-ω SST model consider a fully turbulent boundary layer developed from the flat plate leading edge regardless of freestream turbulent flow intensity. This should not be viewed as a weakness of the model because both are not developed in transition simulation. In contrast, the low-*Re* version of both Menter' s k-ω SST and k-ε models capture the transition zone, but usually predict the onset point much earlier than the reality.

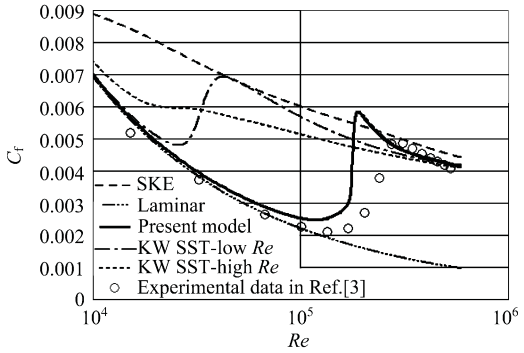

(a) T3A test case

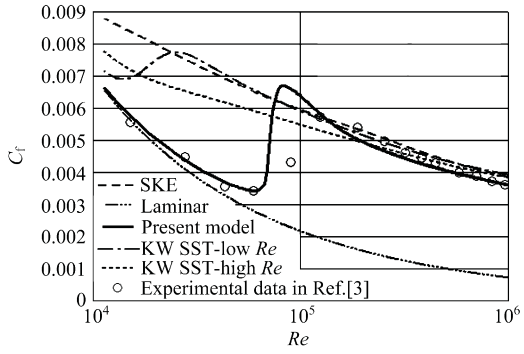

(b) T3B test case

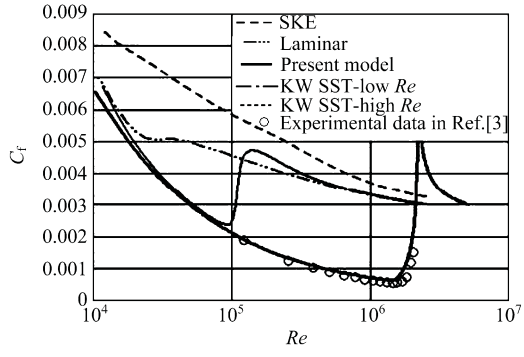

(c) T3A test case

Fig.3 Variation of skin friction coefficients against local Reynolds numbers for flat plate boundary layer flow under zero streamwise pressure gradients.

Fig.4 shows the laminar and turbulent kinetic energy components of the entire fluctuation energy, k_{tot}, at two streamwise positions corresponding to 1.82×10^4 and 9.4×10^5 Reynolds number in the T3B's pre-transitional and fully turbulent regions. In the pre-transitional re-

gion, the laminar fluctuation is of the same order of magnitude as the turbulent fluctuation. In the fully turbulent region, the laminar fluctuation is evidenced very close to the wall because of the similarity between the viscous sub-layer and pre-transitional boundary layer. As seen from Fig.4, a large difference exists in the order of the ratio of k_t/k_l with respect to pre-transitional and fully turbulent regions, which might be ascribed to the transfer of energy between k_l and k_t in transition zone.

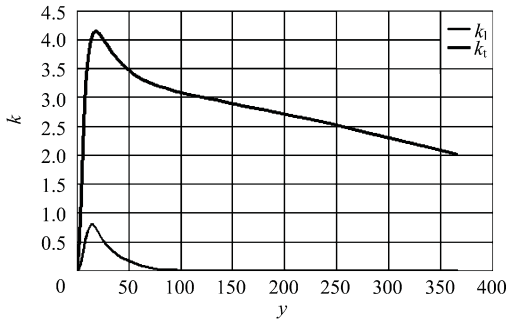

(a) Pre-transitional region

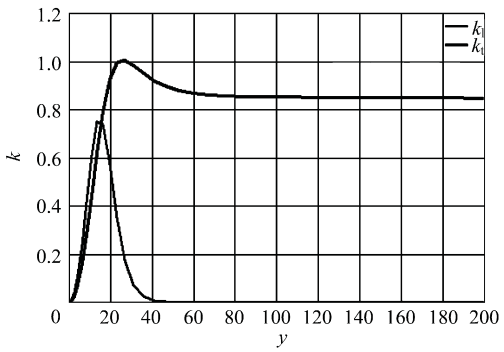

(b) Fully turbulent region

Fig.4 Turbulent and laminar kinetic energy for T3B test case.

Fig.5 illustrates the profiles of non-dimensional laminar kinetic energy, k_l, of pre-transitional boundary layer at four different Reynolds numbers versus non-dimensional wall distance in the T3B test case. Fig.6 shows non-dimensional maximums of laminar kinetic energy, $k_{l,max}$, versus the Reynolds numbers. Both Figs.5-6 clearly display that, at first in pre-transitional region, $k_{l,max}$ grows with Re in an approximate linear manner, then zooms to the maximum in transition zone and ends up saturating. Similar results can be found in M. Matsubara, et al.[13] and P. Luchini[18] works.

Note that in the present model, all of the laminar fluctuation energy components are assumed to be oriented in the streamwise direction. Therefore the total streamwise fluctuation can be expressed by

$$u' = \sqrt{\frac{2}{3}k_t + 2k_l} \tag{14}$$

Fig.7 compares profiles of the non-dimensional total streamwise fluctuation at three different Reynolds numbers with the experimental data of R. E. Mayle, et al.[9] for Tu in the range of 2%-3%. From Fig.7, it is observed that the proposed model reflects pre-transitional fluctuations at levels comparable to those by experiments in flat plate boundary layers.

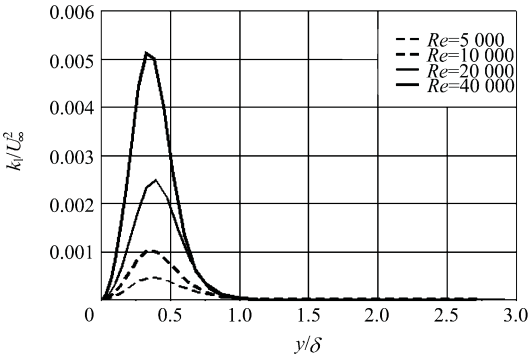

Fig.5 Profiles of non-dimensional laminar kinetic energy in pre-transitional boundary layer at different streamwise Reynolds number positions in T3B test case.

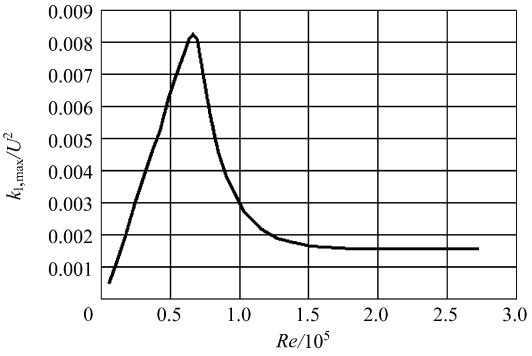

Fig.6 Variation of non-dimensional maximum of laminar kinetic energy against Reynolds number in T3B test case.

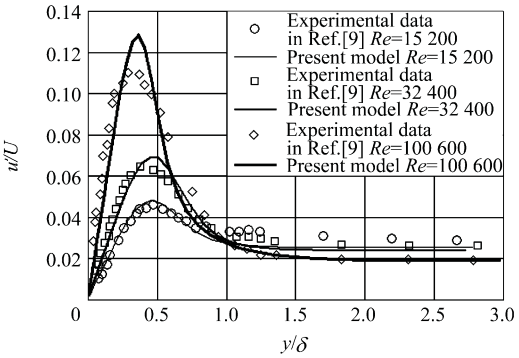

Fig.7 Variation of total streamwise fluctuation for different Reynolds numbers in pre-transitional flat plate boundary layer.

Fig.8 shows the streamwise mean velocity profiles calculated with this model at four downstream positions in comparison with the experimental T3B data. It is clear that the predictions with the model have displayed a perfect agreement with the experimental data even on the detailed mean velocity profiles.

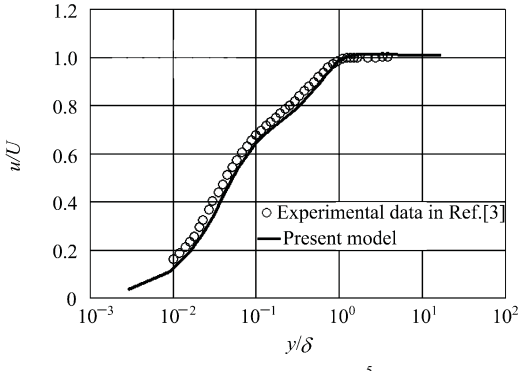

(a) $Re = 2.53\times10^5$

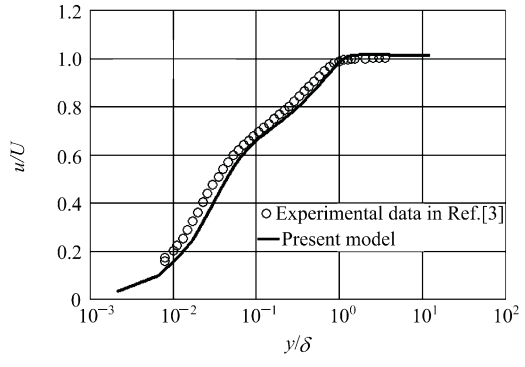

(b) $Re = 3.82\times10^5$

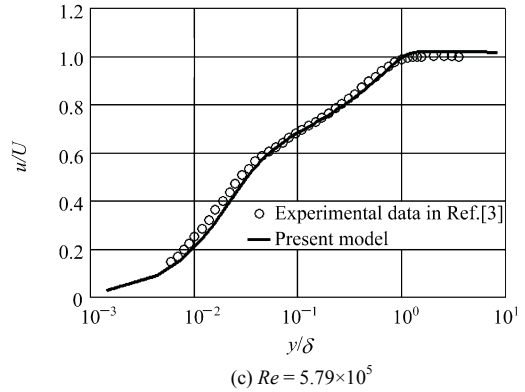

(c) $Re = 5.79\times10^5$

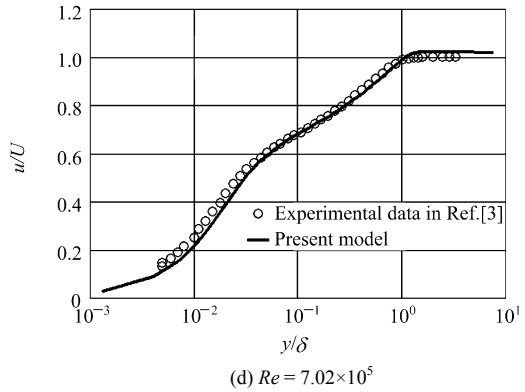

(d) $Re = 7.02\times10^5$

Fig.8 Streamwise mean velocity profiles for T3B test case.

4.2. Flat plate boundary layer under non-zero pressure gradients

Now compare the model predictions in boundary layers under three variable pressure gradients with the ERCOFTAC[3] experimental data and numerical results from the standard k-ε turbulence model. Table 2 lists the inlet conditions of the three cases: freestream turbulence intensity, inlet velocity, and turbulent length scale. For these flows, the pressure gradients are initially negative (favourable) and then positive in a profile that is designed to roughly evaluate the flow over suction side of a gas turbine blade. The streamwise gradient are assumed identical for all three test cases.

Table 2 Inlet flow parameters for flat plate boundary layer flows under non-zero pressure gradient[3]

Test case	Tu/%	U/(m·s^{-1})	λ/mm
T3C1	6.6	5.9	0.6
T3C2	3.0	5.0	0.2
T3C5	3.0	8.4	1.5

Fig.9 shows the skin friction coefficients as a function of downstream Reynolds numbers for three test cases. It is discovered that the model works quite well in predicting the transition locations of these boundary layers under complex variable pressure gradients. Note that, compared to the zero pressure gradient, the initially favourable pressure gradients have got transition delayed. As stated above, since the standard k-ε turbulence model indicates a fully turbulent boundary layer from the leading edge onward, only the turbulent part of this model accords with experimental results.

Fig.10 compares the predictions with Menter's k-ε SST model to the present model in the T3C2 case. As stated in previous cases, the low-Re version of k-ε predicts the transition location earlier than the high-Re version of k-ε.

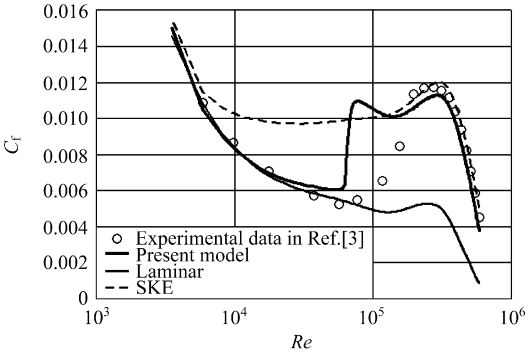

(a) T3C1

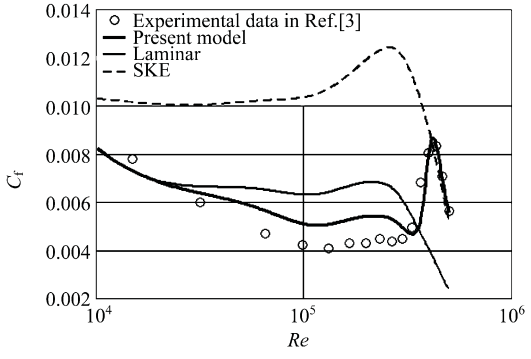

(b) T3C2

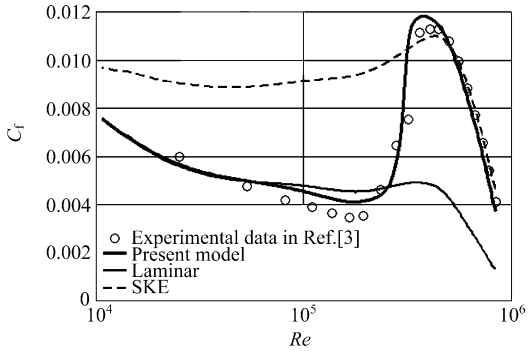

(c) T3C5

Fig.9 Transition in non-zero pressure gradient boundary layer for three cases.

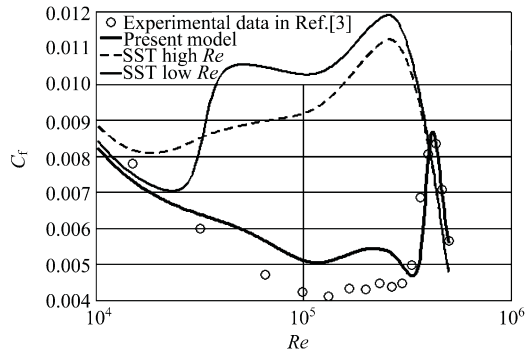

Fig.10 Comparison of Menter's k-ε SST model with present model for T3C2 test case.

4.3. Transitional flow over a wind turbine blade

The last case under study is the flow over the S809 wind turbine blade at 3×10^6 Reynolds number in terms of the blade chord length. In this case, the freestream turbulence intensity is 0.07%. Clearly, for so low a turbulent intensity, natural transition will, more than likely, occur. The flow conditions and the geometry of the blade in this case would surely test on the capability of this model. Fig.11 compares the pressure coefficients obtained with this model to the results with INS2D and standard k-ε model. As expected, it exposes the close analogy between the pressure coefficients obtained with both models.

Fig.12 shows the comparison between the skin friction coefficients and the results with the standard k-ε turbulence model and INS2D[19] code. Note that with the INS2D code, the onset of transition on both sides of the blade is determined manually based on experimental data[20]. It can be observed that the transition location predicted with the proposed model is compatible with the experimental data. Since results with the standard k-ε turbulence model fit in with fully turbulent flows and the model predictions in fully turbulent regions at both sides of the blade are closer to the standard k-ε than the INS2D results, this model is able to make correct prediction of the flow behaviours.

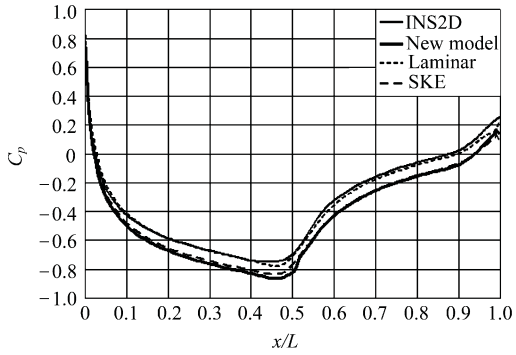

(a) Upper surface

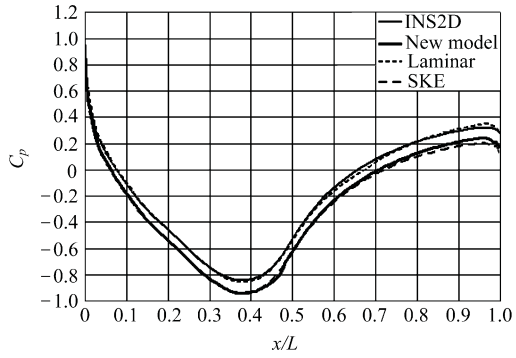

(b) Bottom surface

Fig.11 Pressure coefficient on S809 blade.

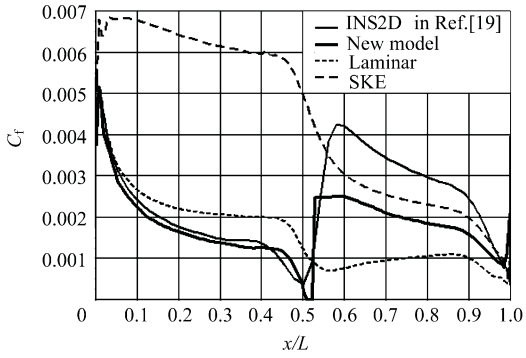

(a) Upper surface

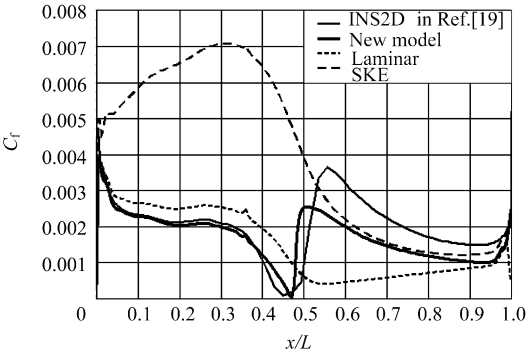

(b) Bottom surface

Fig.12 Transition on S809 blade.

5. Summery and Conclusions

This article has used a new approach based on the

eddy-viscosity RANS equations to predict boundary layer transition. The model involves two major concepts. First, as proposed by R. E. Mayle, et al.[9], a transport equation is used to represent the growth of streamwise fluctuations in the pre-transitional boundary layers. Second, the ideas of P. Bradshow[15] and R. J. Volino[16] are used to grow these streamwise fluctuations through a splat mechanism.

This article has also demonstrated the ability of this model to predict transition in a wide variety of boundary layer flows from natural transition to large free-stream turbulence intensities. The model has been proved to be capable of predicting accurately the transition of flat plate boundary layer flow under favourable and unfavorable pressure gradients and over a wind turbine blade.

One of the main advantages of this model lies in its independence from any modification or users inputting the integral or other non-local parameters. This differs substantially from other existing models, such as F. R. Menter, et al[21-22], which are highly correlated to downstream distance, boundary layer thickness and freestream turbulence intensity. The other advantage is its ease of integration into available in-house or commercial CFD codes.

References

[1] Saric W S. Laminar-turbulent transition: fundamentals. AGARD report No 786, 1992.

[2] Arnal D. Description and prediction of transition in two-dimensional incompressible flow. AGRAD report No 709, 1984.

[3] Coupland J. ERCOFTAC special interest group on laminar to turbulent transition and retransition, T3A and T3B test cases. A309514, 1990.

[4] Savill A M. Some recent progress in the turbulence modelling of bypass transition. In: So R M C, Speziale C G, Launder B E. Near-wall turbulent flows. Elsevier Science Publishers B.V., 1993; 829-848.

[5] Savill A M. One-point closures applied to transition. Turbulence and Transition Modelling. Dordreche: Kluwer Academic Publisher, 1996; 233-268.

[6] Suzen Y B, Huang P G, Hultgren L S, et al. Predictions of separated and transitional boundary layers under low-pressure turbine airfoil conditions using an intermittency transport equation. Journal of Turbomachinery 2003; 125(3): 455-464.

[7] Mayle R E. The role of laminar-turbulent transition in gas turbine engines. ASME Journal of Turbomachinery 1991; 113(4): 509-537.

[8] Abu-Ghannam B J, Shaw R. Natural transition of boundary layers-the effects of turbulence, pressure gradient, and flow history. Journal of Mechanical Engineering Science 1980; 22(5): 213-228.

[9] Mayle R E, Schulz A. The path to predicting bypass transition. ASME Journal of Turbomachinery 1997; 119(3): 405-411.

[10] Walters D K, Leylek J H. A new model for boundary layer transition using a single-point RANS approach. ASME Journal of Turbomachinery 2004; 126(1): 193-202.

[11] Suzen Y B, Huang P G. Modelling of flow transition using an intermittency transport equation. ASME Journal of Fluids Engineering 2000; 122(2): 273-284.

[12] Steelant J, Dick E. Modelling of laminar-turbulent transition for high free-stream turbulence. ASME Journal of Fluids Engineering 2001; 123(1): 22-30.

[13] Matsubara M, Alfredsson P H. Disturbance growth in boundary layers subjected to free-stream turbulence. Journal of Fluid Mechanics 2001; 430; 149-168.

[14] Klebanoff P S. Effects of free-stream turbulence on a laminar boundary layer. Bull Am Phys Soc 1971; 10(11): 1323-1329.

[15] Bradshaw P. Turbulence: the chief outstanding difficulty of our subject. Experimental of Fluids 1994; 16(3-4): 203-216.

[16] Volino R J. A new model for free-stream turbulence effects on boundary layers. ASME Journal of Turbomachinery 1998; 120(3): 613-620.

[17] Menter F R. Two-equation eddy-viscosity turbulence models for engineering applications. AIAA Journal 1994; 32(8): 1598-1605.

[18] Luchini P. Reynolds-number-independent instability of the boundary layer over a flat surface: optimal perturbations. Journal of Fluid Mechanics 2000; 404: 289-309.

[19] Brodeur R. Boundary layer transition prediction for a two dimensional Reynolds averaged Navier-Stokes solver. MS Thesis, University of California, 1997.

[20] Somers D M. Design and experimental results for the S809 airfoil. NREL SR-440-6918, 1997.

[21] Menter F R, Langtry R B, Likki S R, et al. A correlation based transition model using local variables—Part I: model formulation. Journal of Turbomachinery 2006; 128(3): 413-422.

[22] Menter F R, Langtry R B, Likki S R, et al. A correlation based transition model using local variables—Part II: test cases and industrial applications. Journal of Turbomachinery 2006;128(3): 423-434.